Relationship between ENO1 and Metastasis Risk and Prognosis in Esophageal squamous cell carcinoma

Rui Bai
Zhongnan Hospital of Wuhan University
Yuandi Xiang
Renmin Hospital of Wuhan University
Mian Tian
Shenzhen Longhua maternal and Child Health Hospital
Cheng Yuan (yuancheng_89@whu.edu.cn)
Zhongnan Hospital of Wuhan University
Qingquan Hua
Renmin Hospital of Wuhan University

Research Article

Keywords: ENO1, metastasis, ESCC

Posted Date: March 17th, 2022

DOI: https://doi.org/10.21203/rs.3.rs-1454383/v1

Abstract

Objective

Esophageal cancer (EC), a common gastrointestinal malignancy, ranks as the sixth leading cause of cancer death worldwide. Esophageal squamous cell carcinoma (ESCC) is the predominant histological subtype of EC. Lack of potential biomarkers for treatment and prognosis is a limitation for early diagnosis and treatment of ESCC.

Methods

Based on The Cancer Genome Atlas (TCGA) database, the weighted gene co-expression network analysis (WGCNA) was constructed to identify gene modules associated with the metastasis in ESCC. The LASSO algorithm was used to construct a prognosis genes model. After the collinearity test, all independent prognostic parameters and important clinical parameters were included in the prognostic nomogram constructed by the Cox regression model. The nomogram was used to evaluate the prognostic significance of these parameters in ESCC. Finally, we used biological experiments to preliminary investigate the impact of ENO1 on the metastasis risk of ESCC.

Results

A total of 16 genetic modules were identified, and the brown module is considered the most relevant to tumor metastasis. ($P = 0.02$, $R^2 = 0.30$). Protein-protein interaction (PPI) network was performed to identify the hub nodes in the brown module. The univariate and multivariate Cox regression analysis indicated that ENO1 and SUPT5H were independent prognostic factors. Expression data of ENO1 was pipelined along with patients' clinic pathological data for nomogram construction 1-, and 2-OS forecasting. ENO1 gene was regarded as "real" hub genes for cancer metastasis risk. Low-expressed ENO1 inhibited migration and invasion of human ESCC cells in vitro. The mechanism may involve the Wnt signaling pathway and the influence of EMT.

Conclusion

ENO1 might be a novel metastasis risk biomarker for ESCC.

Introduction

Esophageal cancer (EC), a common gastrointestinal malignancy, ranks as the sixth leading cause of cancer death worldwide[1]. Esophageal squamous cell carcinoma (ESCC) is the predominant histological subtype of EC[2]. Surgical resection with lymphadenectomy is the main treatment for ESCC[3]. However,

despite advances in surgical management and multidisciplinary treatment of ESCC, prognosis remains poor[4]. As the most important prognostic factor of esophageal squamous cell carcinoma, lymph node metastasis and distant metastasis are the basis of treatment choice[5]. However, staging components such as lymph node metastasis, invasion depth, and differentiation are not obtained during surgery but commonly determined postoperatively. Therefore, understanding the mechanisms of metastasis of ESCC and potential prognostic molecular markers are urgently required to improve the outcomes for patients with ESCC.

Enolase is a conserved glycolytic enzyme that catalyzes the formation of phosphoenolpyruvate from 2-phosphoglycerides, which is a key step in tumor cell proliferation and metastasis[6,7]. There are three subtypes of ENO, namely ENO-α(ENO-1), ENO-β(ENO-3), ENO-γ(ENO-2). Among them, ENO1 is expressed in almost all tissues of the human body, while ENO2 is mainly expressed in muscle tissues, and ENO3 is mainly expressed in nerve tissues[8]. ENO1 is a multifunctional enzyme, which can be translated into transcription factor MBP-1, which binds to c-MYC-1 in the nucleus. It can also act as a plasminogen receptor to activate plasmin and degrade the extracellular matrix. Previous studies have reported the overexpression of ENO1 in breast cancer, head and neck cancer, lung cancer and gastrointestinal cancer[9–13], which are closely related to cancer progression and poor prognosis. However, there is not enough evidence to indicate that ENO1 is associated with the risk of ESCC metastasis.

In recent years, microarray and high-throughput sequencing technology have been widely applied in biomedical field. However, most studies focus on the screening of differentially expressed genes (DEGs), ignoring the high correlation between genes. Therefore, our study constructed a weighted co-expression network, and then significant hub genes associated with the clinical traits were identified. Finally, it is possible that we identify such biomarkers that can predict the metastasis and progression of ESCC. Our results showed that ENO1 can promote metastasis and progression of ESCC via Wnt signaling pathway.

Methods

Data Collection and Pre-processing

The overall design and procedures are described in a flow chart (Fig. 1). Publicly available mRNA-seq data in ESCC cancer tissue and adjacent noncancerous tissue samples were directly downloaded from the TCGA data portal (http://cancergenome.nih.gov/). We obtained the miRNA profiles of 81 ESCC cancer tissue samples and 1 adjacent noncancerous tissue samples together with the clinical information (level 3) of the corresponding patients. The DEGs were identified by calculating the FC (|log2(FC)| >1 and adjusted P-value < 0.05) with the R package edgeR.

Construction of Weighted Co-expression Network and Division of Co-expression Modules

Firstly, we constructed a Pearson's correlation matrix of all pairwise genes. Secondly, we converted the Pearson's correlation matrix into an adjacency matrix (scale-free network) by the soft-thresholding value. To decide the most appropriate the soft-thresholding value, we calculated the scale-free fit index and mean connectivity. Then, we transformed the adjacency matrix into a topological overlap matrix (TOM) by calculating the topological overlap between pairwise genes, by which we could take indirect correlations into consideration as well as reduce noise and spurious correlations. Finally, we used the average linkage hierarchical clustering based on the TOM-based dissimilarity measure to divide genes into several co-expression modules, so that genes with co-expression relationships were gathered in the same module and genes expressed separately were divided.

Identification of Clinical Significant Modules

Gene significance (GS) and module significance (MS) were used to identify clinical significant modules. The module with the largest absolute MS was generally considered to be a module related to clinical characteristics. Finally, select modules that were highly relevant to certain clinical features for further analysis.

Identification of hub Genes

The hub genes were defined as genes with high module membership (MM) (cor. Weighted > 0.8). Then, the protein–protein interaction (PPI) network was also constructed based on the STRING database (https://string-db.org/). In the PPI network, genes with Top 30 hubba nodes ranked by Maximal Clique Centrality (MCC) were also defined as hub genes. The common hub genes in both co-expression networks and PPI networks were regarded as "real" hub genes for further analyses.

Construction of a prognosis genes model

After filtration of hub Genes through WCGNA and PPI, candidate prognostic genes were selected via integrated analysis of two algorithms consisting of the LASSO algorithm with penalty parameter tuning conducted, and the SVM-RFE algorithm searching for lambda with the smallest classification error to determine the variable. According to the optimal cut-off value of prognostic genes, patients were divided into high-risk group and low-risk group. A multivariate Cox regression model was finally used to construct a prognostic signature based on the candidate genes generated from the above filtration. A receiver operating characteristic (ROC) curve was used to estimate the accuracy and efficiency of the signature in a time-dependent manner.

Predictive Nomogram Construction

In order to determine the independent prognostic value of genes and clinic pathological parameters (including age, gender, TNM staging) in the TCGA dataset. $P < 0.05$ was considered statistically significant. After the collinearity test, all independent prognostic parameters and important clinical parameters were included in the prognostic nomogram constructed by the Cox regression model. The nomogram was used to evaluate the prognostic significance of these parameters in ESCC. The nomogram calibration curve was used to compare predicted and observed overall survival rates. According to the total score of the nomogram, the best cut-off value of RiskScore was calculated. According to the RiskScore, and the patients were divided into high or low group. The survfit function was further evaluated to analyze the prognostic by logrank. The 1-year, and 3-year AUC were analyzed by pROC package.

ESCC cell lines and siRNA infection

ESCC cell lines including TE-1, KYSE150 and KYSE520 were cultured in DMEM medium (Gibco, Carlsbad, CA, USA) supplemented with 10% fetal bovine serum (FBS) (Gibco, Carlsbad, CA, USA). To establish transfectants with ENO1 knockdown, TE-1 and KYSE150 were transfected with siRNAs (target sequence for siENO1-1#: 5'-GCCAUGCCAGGGAGAUCUUUTT-3', siENO1-2#:5'-GCUGGCAACUCUGAAGUCATT-3', siENO1-3#: 5'- CCCAGUGGUGUCUAUCGAATT-3'). The transfection was performed using jetPEI (Dakewei, China).

Quantitative real-time PCR assay (qRT-PCR)

Total RNA from cell lines was isolated by a trizol agent and reverse transcribed to synthesize complementary DNA (cDNA) by the RevertAid First Strand cDNA Synthesis Kit. We performed the qRT-PCR with SYBR Green Mix in the RT-PCR detection system (Bio-Rad, USA) based on the manufacturer's protocols. The relative mRNA expression of ENO1 was measured by $2\text{-}\Delta\Delta Ct$ methods and the GAPDH was served as an internal control. The primers involved in our study are as follows:

ENO1 forward:5'- AGTCTACGGGACCGAAAGACA – 3'

ENO1 reverse: 5'- CAGACCTTGCAGTTCGTTCAG – 3'

GAPDH forward: 5'- GGACCTGACCTGCCGTCTAG – 3'

GAPDH reverse: 5'- GTAGCCCAGGATGCCCTTGA – 3'

Cell proliferation assay

The transfected cells were plated in 96-well plates at 10^4 cells per well with 100 µl of culture medium in a humidified condition at 37 ℃. Then, 10 µl CCK-8 solutions were added into each well and further

incubated in humidified condition at 37 ℃ for 1 h. Finally, the cells were measured at the absorbance of 450 nm according to the indicated time point. Each experiment was repeated at least three times.

Cell migration and invasion assay

As for the cell migration experiment by wound healing assay, the cells were sowed in 6-well plates with serum-free culture medium (10^6 cell/well). The scratch was formed by the tip of a 200 μl plastic pipette. After 48 hours, the migrated cells were washed with phosphate buffer solution (PBS) and fixed with 4% paraformaldehyde. The migration distance was calculated under an optical microscope.

As for invasion assay through the 8- um chamber. Firstly, the chamber was pretreated with matrigel. Then, 5×10^4 cells were seeded into the serum-free upper chamber, while medium with 10% FBS was added to the lower chamber. After 24 hours, the subsurface migrating cells will be washed with PBS, fixed with 4% paraformaldehyde and stained with crystal violet solution. The invasion capability was determined by calculating the migrating cells on the sub-surface through an optical microscope.

Western blot assay

Total protein was extracted with RIPA buffer containing protease and phosphatase inhibitor. After being blocked, the membranes were incubated with the primary antibody for 1 h at room temperature. Then, the membranes were incubated with secondary antibodies at room temperature for 1 h. The protein bands were visualized using enhanced chemiluminescence chromogenic substrate with horseradish peroxidase.

Statistical analysis

All statistical analysis was conducted with SPSS 21.0 and the results in our study were expressed as mean ± SD. The significance of the changes between the two groups was determined by Student's t-test, and the data were considered significant when $P < 0.05$.

Results

DEGs screening

Under the threshold of $|\log_2(FC)| > 1$ and adjusted P-value < 0.05, a total of 154 DEGs (88 up-regulated and 66 down-regulated in ESCC) were selected (Fig. 1A). The DEGs and clustering dendrogram of tumor samples, as well as the clinical traits were shown in Fig. 1B.

Co-expression network construction and key modules identification

Using the “WGCNA” package in R, the genes that expression variance was greater than the quartile of all variances were grouped into modules. Here, the power of β = 5 (scale free R^2 = 0.84) was selected as the soft-thresholding to ensure a scale-free network (Fig. 2). Sixteen modules are considered to be significantly correlated (Fig. 3). And the correlation between the brown module and metastasis risk was high (P = 0.02, R^2 = 0.30) (Fig. 4A). Thus, the brown module with metastasis risk was identified as the clinical significant module.

Identification of hub genes for metastasis risk in the brown module

The highly linked hub genes in the module act as key functions in biological processes. Therefore, in the brown module, genes with high connectivity (weighted correlation coefficient > 0.8) were selected as the candidate hub genes for the metastasis risk of the module. Furthermore, we also constructed a network of PPI (Fig. 4B),

Construction of a prognostic model from the TCGA cohort

The top 30 hubba nodes were identified based on Maximal Clique Centrality (MCC) through Cytohubba plug-in. LASSO Cox regression was utilized to evaluate prognostic genes in ESCC patients. Prognosis related genes were identified based on the optimal value of λ and subsequently used to construct an all subset regression model (Fig. 5A**)**. The risk score for prognostic prediction was calculated as follows: Riskscore = (0.1623)*ENO1+(-0.1131)*OPRD1+(-0.0103)*TAF13+(-0.3686)*SUPT5H. Patients were divided into high-risk group and low-risk group using Riskscore median value (Fig. 5B), and OS of the high-risk group was significantly shorter than that of the low-risk group (HR = 2.425, 95%CI: 1.231–4.777, P = 0.0104, Fig. 5C). In addition, the AUCs for 1-, 2-, and 3-year overall survival predictions for the risk scores were 0.675, 0.759 and 0.777, respectively (Fig. 5D).

Establishment of a prognostic gene nomogram

In the TCGA dataset, univariate Cox regression analysis demonstrated that pathologic gender, ENO1 and SUPT5H had prognostic value (Fig. 6A). Multivariate Cox regression analysis indicated that ENO1 and SUPT5H were independent prognostic factors (Fig. 6B).

Expression data of ENO1 and SUPT5H was pipelined along with patients’ clinic pathological data for nomogram construction 1-, and 2-OS forecasting. The results also supported ENO1 and SUPT5H were independent prognostic factors related to OS, and ENO1 was a risk prognostic factor (Fig. 6C). The calibration plot (Fig. 7A) of the nomogram indicated optimal predictive accuracy, with a close overlap between predicted and actual OS. The AUCs for 1- and 2- OS predictions for the risk scores were 0.78 and

0.84, respectively (Fig. 7B). High-risk groups had markedly poorer outcomes than low-risk groups (Fig. 7C).

Hub gene validation

The expression of ENO1 in ESCC tumor tissue was significantly lower than that in normal tissue (Fig. 8A), which was verified by ESCC cell lines (TE-1, KYSE150 and KYSE520) compared with the normal human esophageal epithelial cells (HEEC) (Fig. 8B). Meanwhile, we also found a poorer survival rate in the samples with high expression levels of ENO1 (HR = 2.34, 95%CI: 1.02–5.37, P = 0.038; Fig. 8C).

Low-expressed ENO1 inhibited cell migration and invasion

As shown in Fig. 9, the migration capacity of TE-1 and KYSE150 cells was inhibited in the ENO1-downregulated group compared with that in the control group by wound healing assay. Besides, the invasive capacity was repressed in the ENO1-downregulated group compared with that in the control group by the transwell assay. These data indicated that low-expressed ENO1 could inhibite the capacity of migration and invasion in ESCC cell lines.

The relationship between ENO1, EMT and Wnt signal pathway

KEGG enrichment analysis showed that the hub genes were enriched in Wnt/β-catenin signal pathway (Fig. 10A). ENO1 silencing inhibited the protein level of N-cadherin, vimentin and enhance the protein level of E-cadherin. To explore the underlying mechanisms that contribute to the effects of ENO1 in ESCC, we analyzed Wnt signal pathway related proteins. We found that the downregulation of ENO1 reduced the protein of β-catenin, cmyc, cyclinD1. These results indicated that ENO1 promoted EMT of ESCC via the Wnt signal pathway (Fig. 10B).

Discussion

In this study, we validated gene co-expression modules related to the metastasis risk and prognosis of ESCC by WGCNA. The hub genes were significantly correlated with the metastasis risk. ENO1 was most highly correlated with metastasis risk in ECSS patients. The present study, based on TCGA data, revealed that ENO1 was over-expressed in ECSS tissue samples, and ECSS patients with high-expressed ENO1 did not benefit from survival compared with patients with low-expressed ENO1. Then single gene GSEA analysis showed that the ENO1 gene was mainly enriched in the Wnt signaling pathway in ESCC. Thus,

we speculated that ENO1 might affect the metastasis risk and prognosis of ESCC patients via the Wnt signaling pathway.

Many studies have shown that ENO1 is highly expressed in malignant tumors. Relevant researches show that silencing ENO1 can inhibit the occurrence, migration, invasion and metastasis of colorectal cancer, breast cancer, non-small cell lung cancer, glioma and endometrial cancer[14–18]. As a multifunctional protein, ENO1 plays an important role in the occurrence and development of tumors by acting as an enzyme and plasminogen receptor. On the one hand, in the final step of the glycolytic pathway, ENO1 acts as an enzyme to maintain aerobic glycolysis[19]. On the other hand, on the surface of cancer cells, ENO1 acts as a plasminogen receptor and participates in the degradation of the extracellular matrix by promoting the activation of plasminogen to plasmin and is beneficial to cell invasion and metastasis[20,21]. Therefore, it plays a key role in cancer proliferation, metastasis and spread[22,23]. Studies have found that the up-regulation of ENO1 in a variety of tumors is related to the shorter survival time of patients. In our study, we found that ENO1 silencing inhibited the migration and invasion of ESCC.

Some studies have reported that the possible mechanisms involved in ENO1 induced metastasis include the P13K/AKT pathway and its downstream signals [24] (including glycolysis, cell cycle progression and epithelial-mesenchymal transition related genes). Our bioinformatics results showed that ENO1 was involved in the Wnt signaling pathway in ESCC.

Wnt signaling has important physiological functions. In the early embryonic growth and development process, Wnt signaling pathway is a necessary factor for the formation of the brain and nervous system[25,26]. At the same time, Wnt signaling is also closely related to stem cell self-renewal and differentiation regulation. Wnt signaling pathway is of great significance for the self-renewal of hematopoietic stem cells. It also maintains the stability of the small intestine tissue, regulates bone density and the differentiation of adipocytes[27]. However, the dysregulation of the Wnt signal transduction pathway is related to a variety of known high-incidence carcinogenesis[28]. According to different ways of signal transduction by Wnt protein, Wnt signal transduction can be divided into the canonical Wnt signal pathway and the non-canonical Wnt signaling pathway. Some studies have demonstrated that the Wnt signal pathway is involved in proliferation and migration of ESCC[29–31]. In recent years, studies have found that both the canonical and the non-canonical Wnt signal pathways are involved in the induction of EMT. There are sometimes crosstalks between different Wnt signaling pathway and between Wnt signaling and other pathways which makes the molecular mechanism more complicated. In our study, we found that downregulation of the ENO1 inactivates the Wnt signaling pathway.

It is undeniable that our experiment has certain flaws. First of all, the mechanism needs to be more in-depth. Second, our research lacks overall clinical samples and animals. But in general, our research initially verified that ENO1 promotes migration and invasion of ESCC via the Wnt signaling pathway.

In conclusion, we predicted that ENO1 might affect the metastasis risk and prognosis of ESCC patients through bioinformatics, and then verified it at the cytological level. Through our research, we found that

this gene can affect the migration and invasion of ESCC via the Wnt signaling pathway.

Declarations

Acknowledgments

Not applicable.

Consent for publication

We confirm that the manuscript has been read and approved by all named authors and that there are no other persons who satisfied the criteria for authorship but are not listed. We further confirm that the order of authors listed in the manuscript has been approved by all of us.

Ethics approval and consent to participate

Not applicable.

Consent for publication

Not applicable.

Data Availability Statement

The data used to support the findings of this study are available from the corresponding author upon request.

Competing interests

The authors declare that they have no competing interests.

Founding

None

Authors' contributions

QQH and CY conceived and designed the experiments, RB and YDX performed the experiments. All authors read and approved the final manuscript.

References

1. Fitzmaurice C, Abate D, Abbasi N, et al. Global, Regional, and National Cancer Incidence, Mortality, Years of Life Lost, Years Lived With Disability, and Disability-Adjusted Life-Years for 29 Cancer

Groups, 1990 to 2017: A Systematic Analysis for the Global Burden of Disease Study. *JAMA oncology.*2019;5(12):1749-1768.

2. Malhotra GK, Yanala U, Ravipati A, Follet M, Vijayakumar M, Are C. Global trends in esophageal cancer. 2017;115(5):564-579.
3. Fujiwara Y, Yoshikawa R, Kamikonya N, et al. Neoadjuvant chemoradiotherapy followed by esophagectomy vs. surgery alone in the treatment of resectable esophageal squamous cell carcinoma. *Molecular and clinical oncology.*2013;1(4):773-779.
4. Sohda M, Kuwano H. Current Status and Future Prospects for Esophageal Cancer Treatment. *Annals of thoracic and cardiovascular surgery : official journal of the Association of Thoracic and Cardiovascular Surgeons of Asia.*2017;23(1):1-11.
5. Rice TW, Ishwaran H, Hofstetter WL, Kelsen DP, Apperson-Hansen C, Blackstone EH. Recommendations for pathologic staging (pTNM) of cancer of the esophagus and esophagogastric junction for the 8th edition AJCC/UICC staging manuals. *Diseases of the esophagus : official journal of the International Society for Diseases of the Esophagus.*2016;29(8):897-905.
6. Zhu X, Miao X, Wu Y, et al. ENO1 promotes tumor proliferation and cell adhesion mediated drug resistance (CAM-DR) in Non-Hodgkin's Lymphomas. *Experimental cell research.*2015;335(2):216-223.
7. Kang HJ, Jung SK, Kim SJ, Chung SJ. Structure of human alpha-enolase (hENO1), a multifunctional glycolytic enzyme. *Acta crystallographica Section D, Biological crystallography.*2008;64(Pt 6):651-657.
8. Lebioda L, Stec B. Crystal structure of enolase indicates that enolase and pyruvate kinase evolved from a common ancestor. *Nature.*1988;333(6174):683-686.
9. Tu SH, Chang CC, Chen CS, et al. Increased expression of enolase alpha in human breast cancer confers tamoxifen resistance in human breast cancer cells. *Breast cancer research and treatment.*2010;121(3):539-553.
10. Tsai ST, Chien IH, Shen WH, et al. ENO1, a potential prognostic head and neck cancer marker, promotes transformation partly via chemokine CCL20 induction. *European journal of cancer (Oxford, England : 1990).*2010;46(9):1712-1723.
11. Pernemalm M, De Petris L, Branca RM, et al. Quantitative proteomics profiling of primary lung adenocarcinoma tumors reveals functional perturbations in tumor metabolism. *Journal of proteome research.*2013;12(9):3934-3943.
12. Bai Z, Ye Y, Liang B, et al. Proteomics-based identification of a group of apoptosis-related proteins and biomarkers in gastric cancer. *International journal of oncology.*2011;38(2):375-383.
13. Cheng Z, Shao X. ENO1 Acts as a Prognostic Biomarker Candidate and Promotes Tumor Growth and Migration Ability Through the Regulation of Rab1A in Colorectal Cancer. 2019;11:9969-9978.
14. Principe M, Ceruti P, Shih N-Y, et al. Targeting of surface alpha-enolase inhibits the invasiveness of pancreatic cancer cells. *Oncotarget.*2015;6(13):11098-11113.
15. Zhao M, Fang W, Wang Y, et al. Enolase-1 is a therapeutic target in endometrial carcinoma. *Oncotarget.*2015;6(17):15610-15627.

16. Song Y, Luo Q, Long H, et al. Alpha-enolase as a potential cancer prognostic marker promotes cell growth, migration, and invasion in glioma. *Mol Cancer.*2014;13:65.
17. Fu Q-F, Liu Y, Fan Y, et al. Alpha-enolase promotes cell glycolysis, growth, migration, and invasion in non-small cell lung cancer through FAK-mediated PI3K/AKT pathway. *J Hematol Oncol.*2015;8:22.
18. Capello M, Ferri-Borgogno S, Riganti C, et al. Targeting the Warburg effect in cancer cells through ENO1 knockdown rescues oxidative phosphorylation and induces growth arrest. *Oncotarget.*2016;7(5):5598-5612.
19. Warburg O, Wind F, Negelein E. THE METABOLISM OF TUMORS IN THE BODY. *J Gen Physiol.*1927;8(6):519-530.
20. Pancholi V. Multifunctional alpha-enolase: its role in diseases. *Cell Mol Life Sci.*2001;58(7):902-920.
21. López-Pedrera C, Villalba JM, Siendones E, et al. Proteomic analysis of acute myeloid leukemia: Identification of potential early biomarkers and therapeutic targets. *Proteomics.*2006;6 Suppl 1:S293-S299.
22. Ceruti P, Principe M, Capello M, Cappello P, Novelli F. Three are better than one: plasminogen receptors as cancer theranostic targets. *Exp Hematol Oncol.*2013;2(1):12.
23. Capello M, Ferri-Borgogno S, Cappello P, Novelli F. α-Enolase: a promising therapeutic and diagnostic tumor target. *FEBS J.*2011;278(7):1064-1074.
24. Wang G, Yu Y, Wang Y-Z, Yin P-H, Xu K, Zhang H. The effects and mechanisms of isoliquiritigenin loaded nanoliposomes regulated AMPK/mTOR mediated glycolysis in colorectal cancer. *Artif Cells Nanomed Biotechnol.*2020;48(1):1231-1249.
25. Wang Y-Z, Molotkov A, Song L, Li Y, Pleasure DE, Zhou C-J. Activation of the Wnt/beta-catenin signaling reporter in developing mouse olfactory nerve layer marks a specialized subgroup of olfactory ensheathing cells. *Dev Dyn.*2008;237(11):3157-3168.
26. Fossat N, Jones V, Khoo P-L, et al. Stringent requirement of a proper level of canonical WNT signalling activity for head formation in mouse embryo. *Development.*2011;138(4):667-676.
27. Ghosh N, Hossain U, Mandal A, Sil PC. The Wnt signaling pathway: a potential therapeutic target against cancer. *Ann N Y Acad Sci.*2019;1443(1):54-74.
28. Lie D-C, Colamarino SA, Song H-J, et al. Wnt signalling regulates adult hippocampal neurogenesis. *Nature.*2005;437(7063):1370-1375.
29. Ma J, Zhang Y, Deng H, et al. Thymoquinone inhibits the proliferation and invasion of esophageal cancer cells by disrupting the AKT/GSK-3β/Wnt signaling pathway via PTEN upregulation. *Phytother Res.*2020.
30. Han S, Wang Y, Ma J, Wang Z, Wang H-MD, Yuan Q. Sulforaphene inhibits esophageal cancer progression via suppressing SCD and CDH3 expression, and activating the GADD45B-MAP2K3-p38-p53 feedback loop. *Cell Death Dis.*2020;11(8):713.
31. Zhang L-N, Zhao L, Yan X-L, Huang Y-H. Loss of G3BP1 suppresses proliferation, migration, and invasion of esophageal cancer cells via Wnt/β-catenin and PI3K/AKT signaling pathways. *J Cell*

*Physiol.*2019;234(11):20469-20484.

Figures

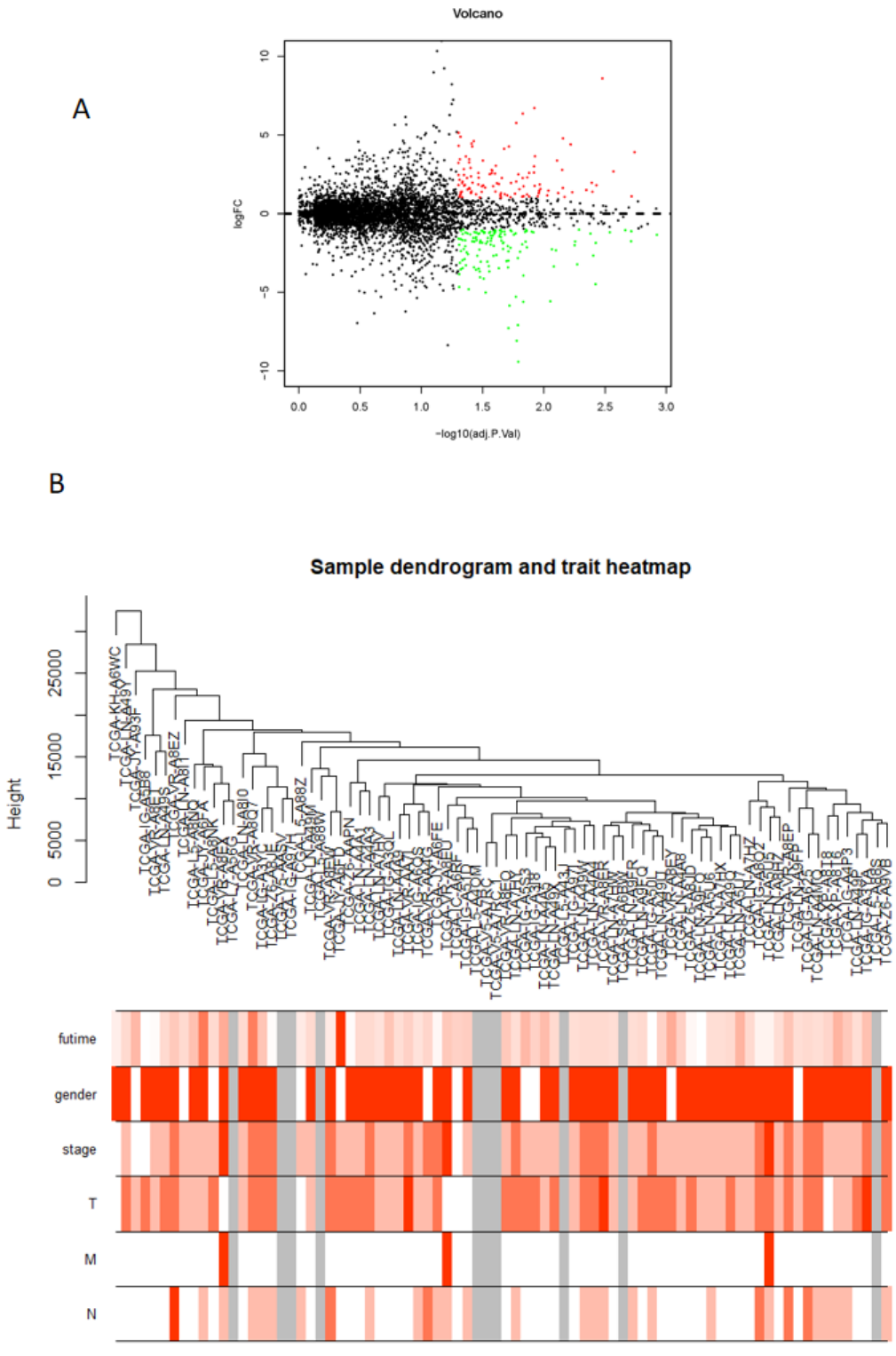

Figure 1

The differentially expressed genes (DEGs) and clustering dendrogram of tumor samples, as well as the clinical traits. (A) The volcano plot for all DEGs. (B) The clustering was based on DEGs between ESCC and normal.

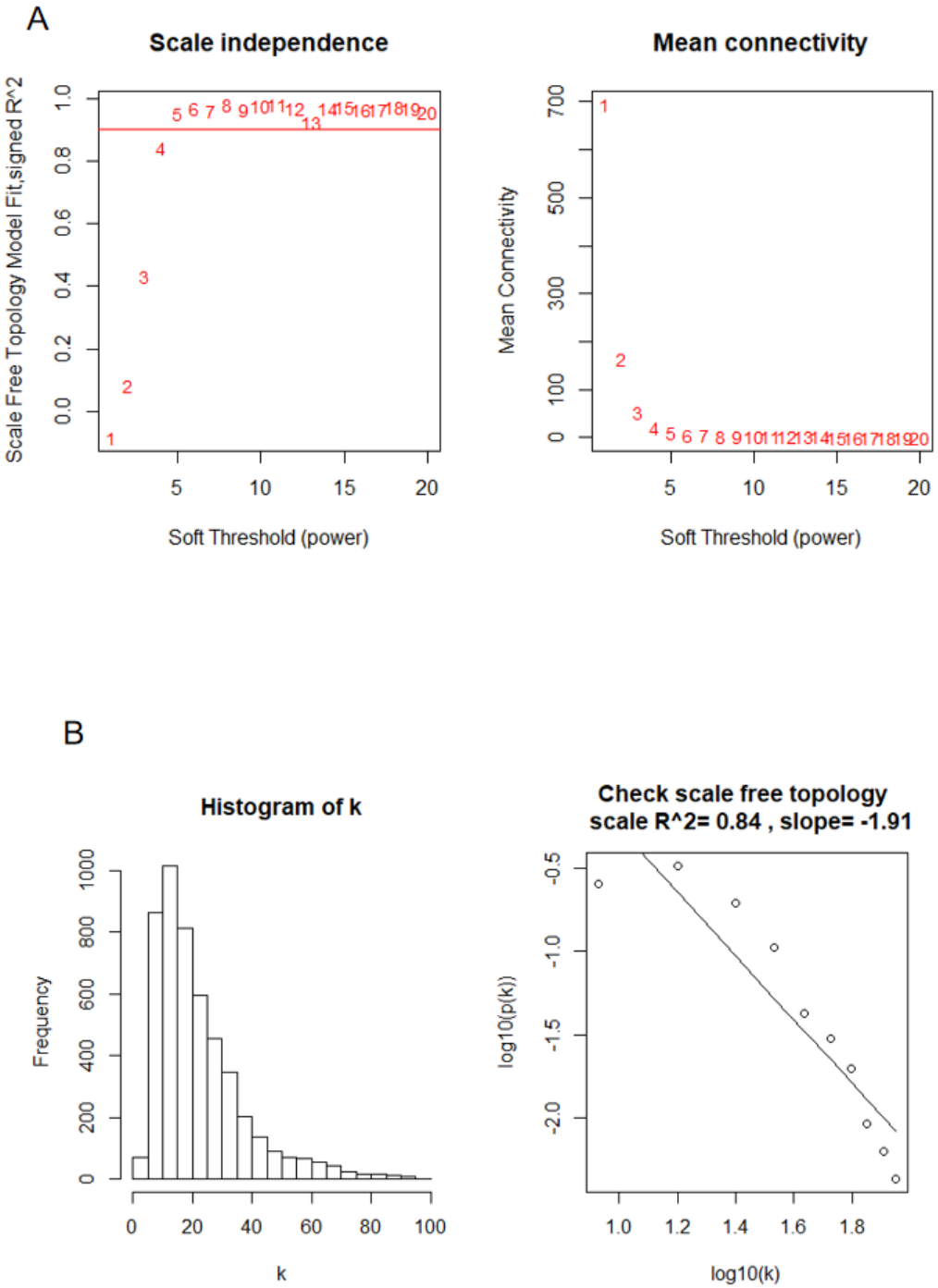

Figure 2

Determine soft-thresholding power in WGCNA.

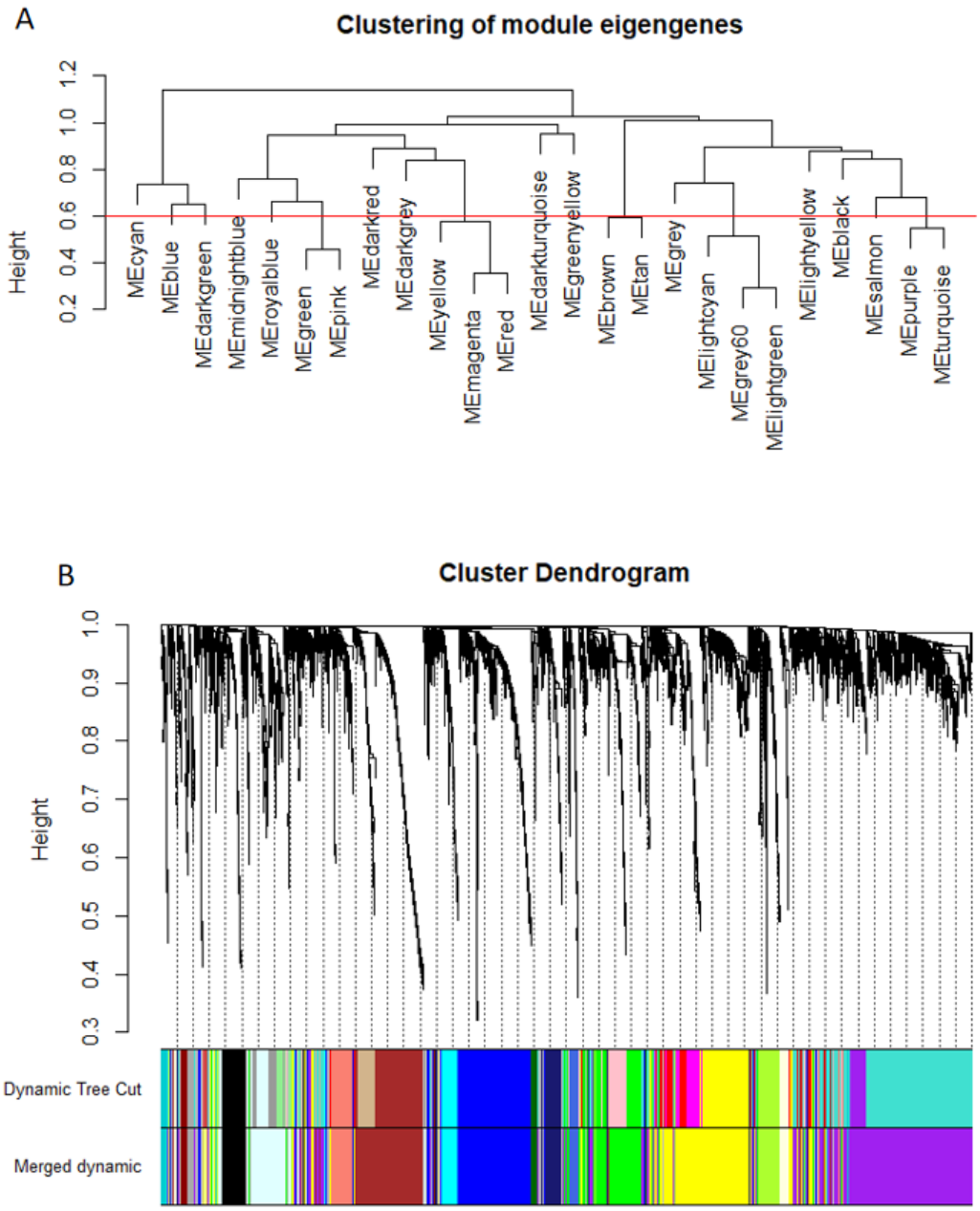

Figure 3

Identifying modules associated with the clinical traits of ESCC.

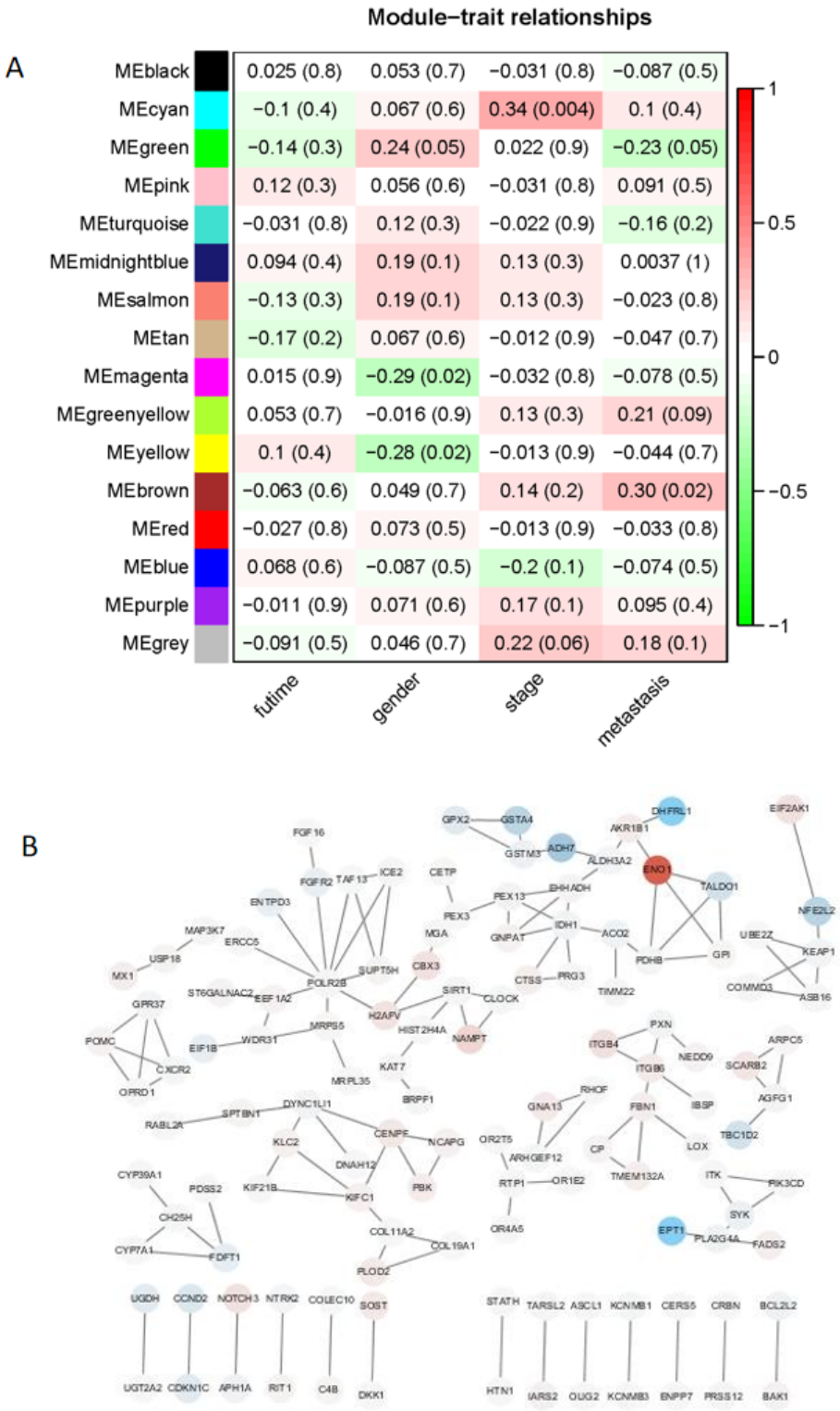

Figure 4

The hub genes module and PPI network. (A) Heatmap of the correlation between module eigengenes and clinical traits of ESCC; (B) PPI network of genes in the brown module.

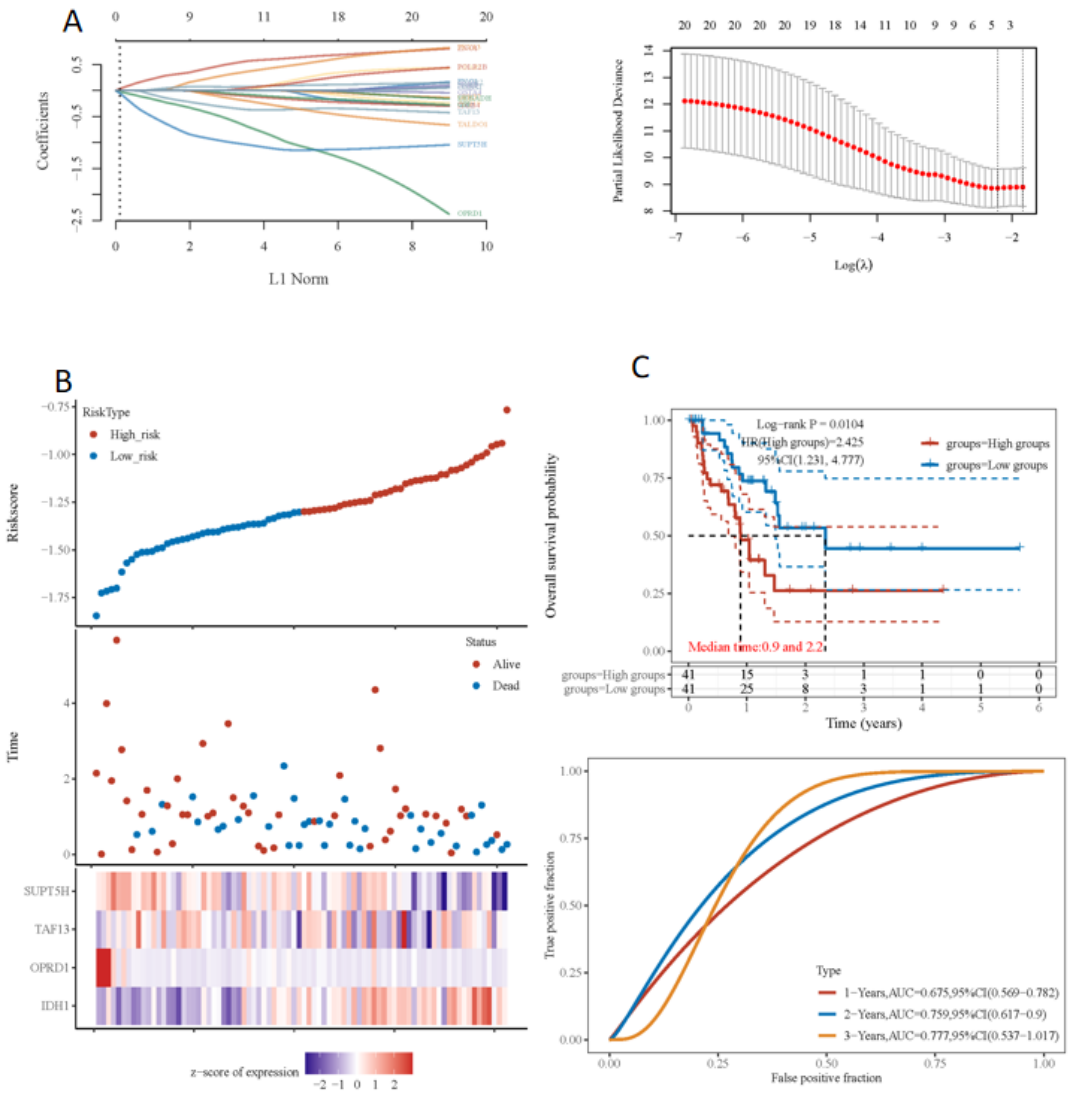

Figure 5

Construction of a prognostic model from the TCGA cohort. **(A)** LASSO coefficient profiles of hub genes; (B) The risk plot of OS predictive model in TCGA; (C) Overall survival curve between high-risk group and low-risk group (D) ROC curve of 1-. 2- and 3-year.

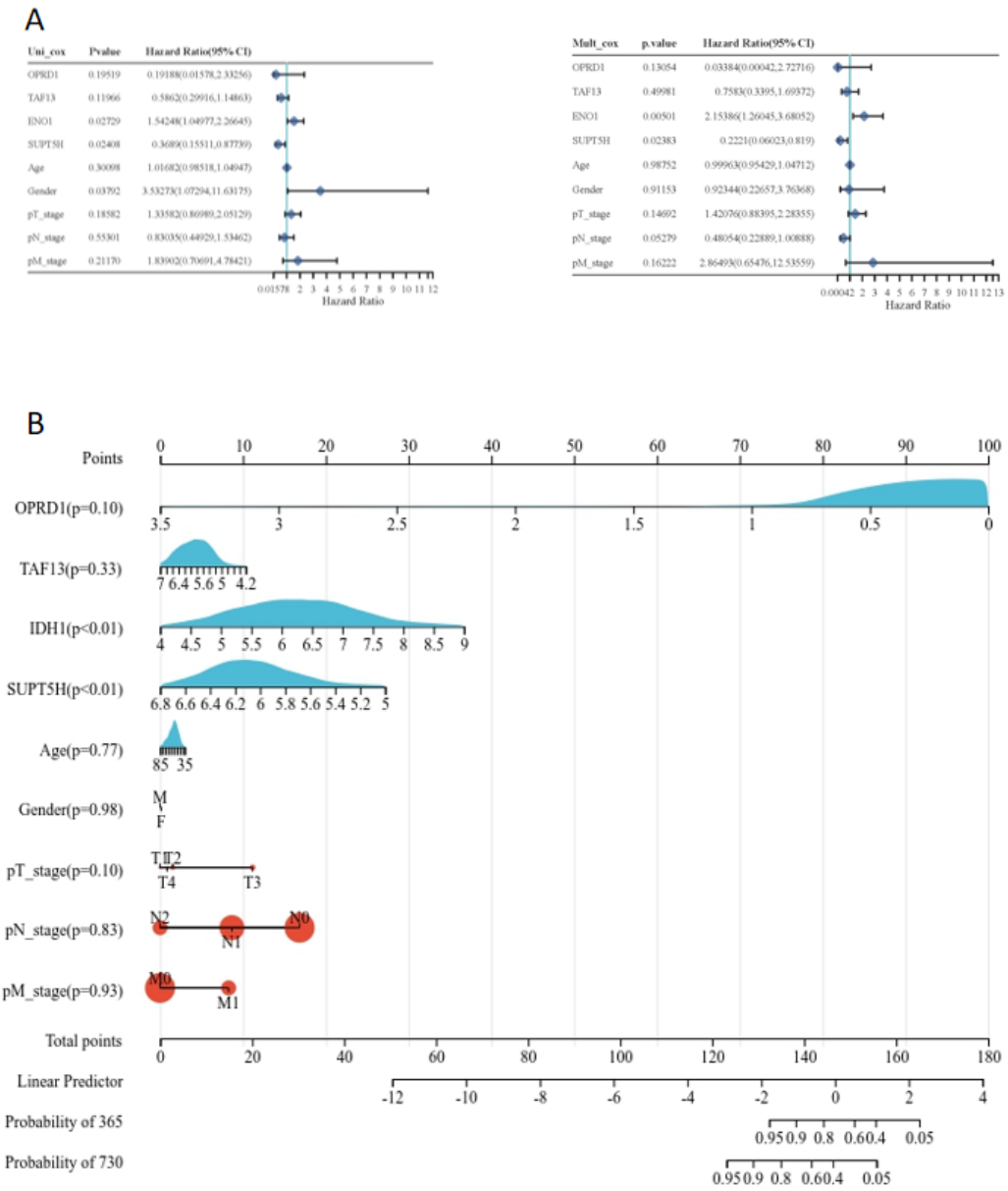

Figure 6

Construction of a nomogram based on clinical information. (A) Univariate Cox regression analysis and Multivariate Cox regression analysis; (B) The nomogram plot.

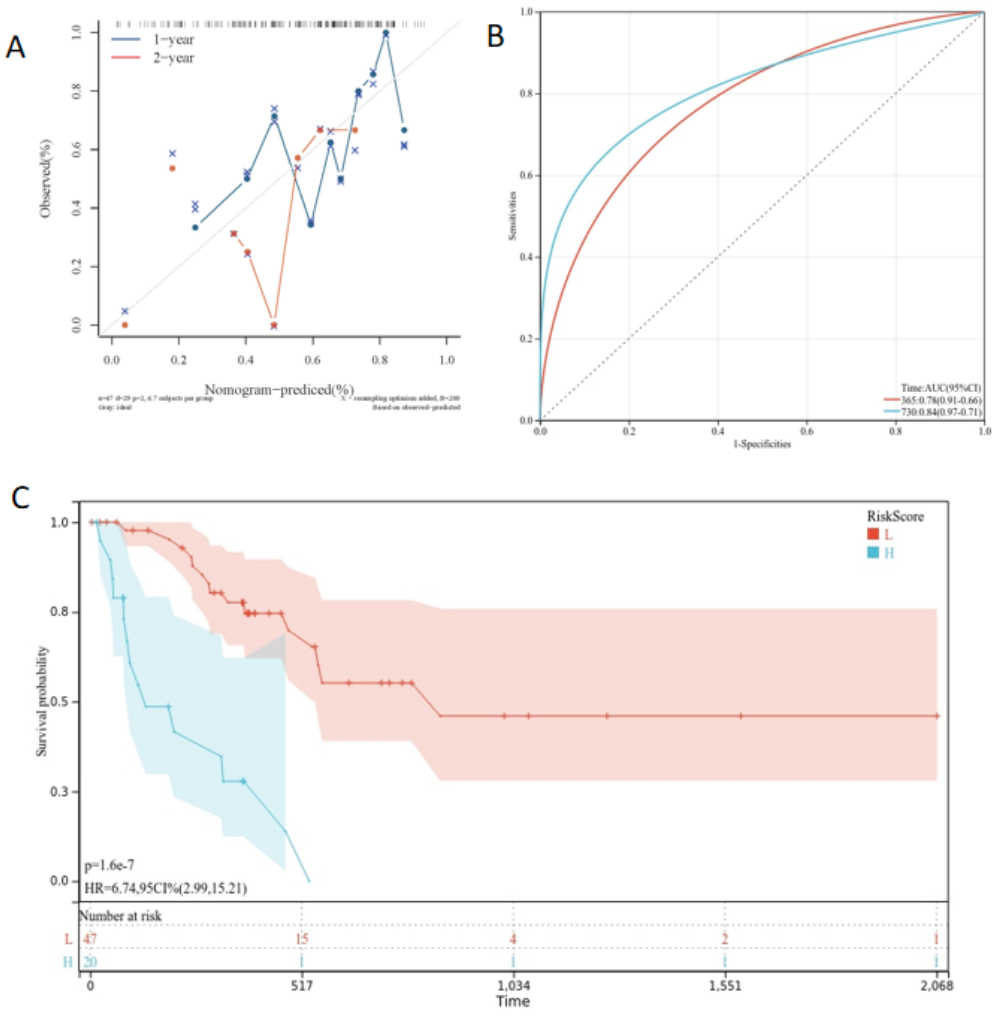

Figure 7

Construction of a nomogram based on clinical information. (A) the calibrations of 1 and 2 years; (B) ROC curve of established nomogram; (C) Kaplan-Meier curve of established nomogram

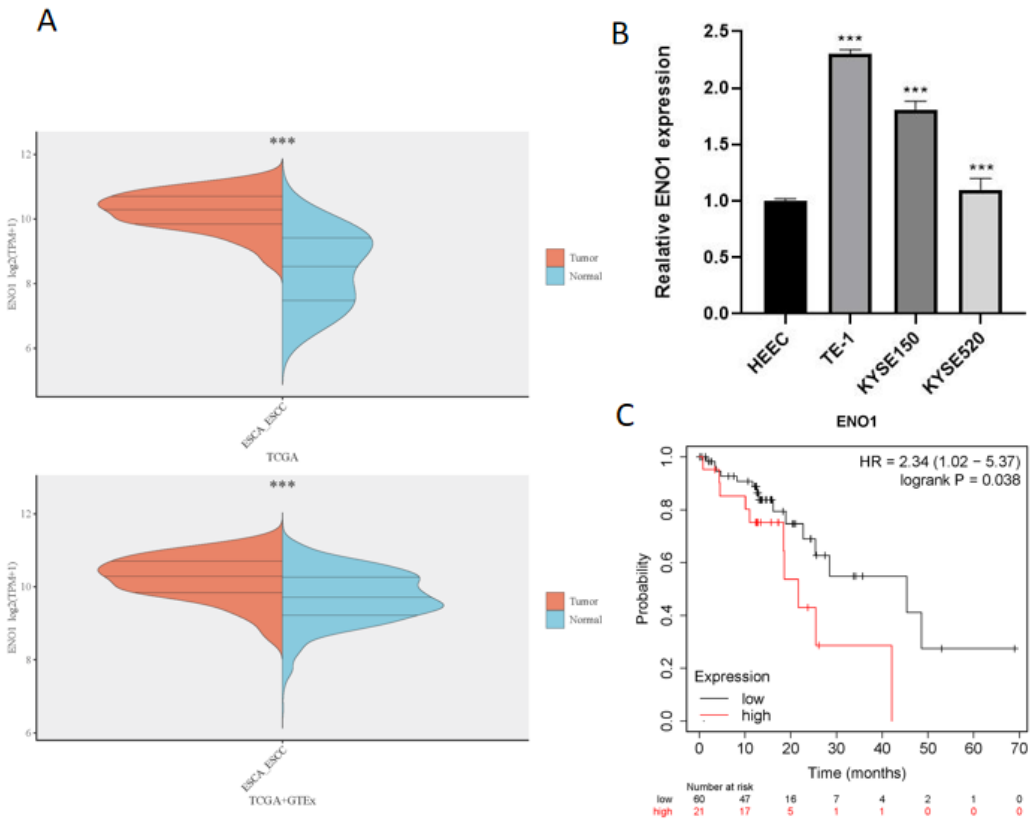

Figure 8

Validation of hub gene. (A) Differential expression of ENO1 gene in ESCC tissues and normal tissues based on TCGA and GTEx; (B) Quantitative RT-PCR analysis of ENO1 expression in HEEC and ESCC cell lines; (C) Kaplan-Meier plot of overall survival for ENO1 expression.

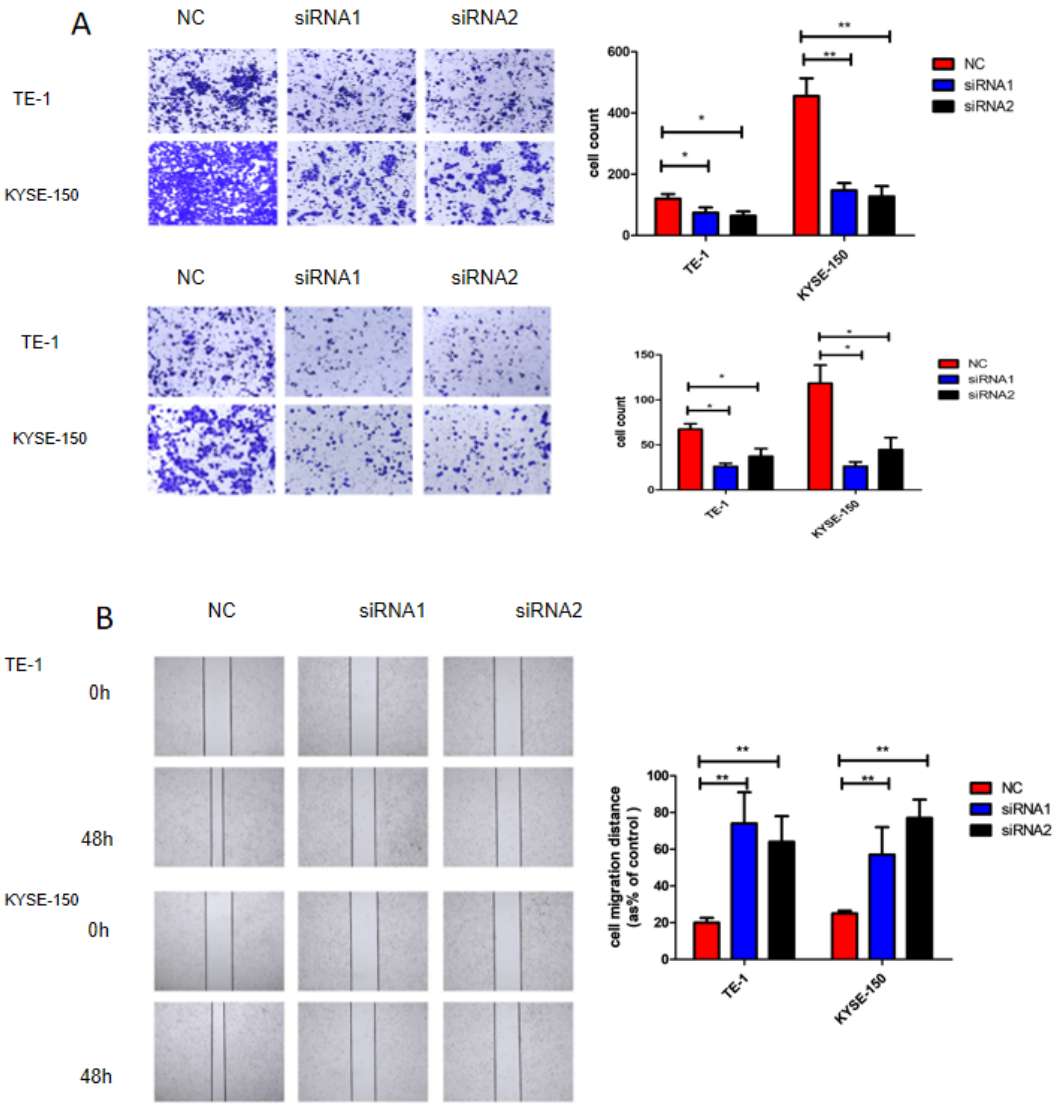

Figure 9

Low-expressed ENO1 inhibited cell migration and invasion.

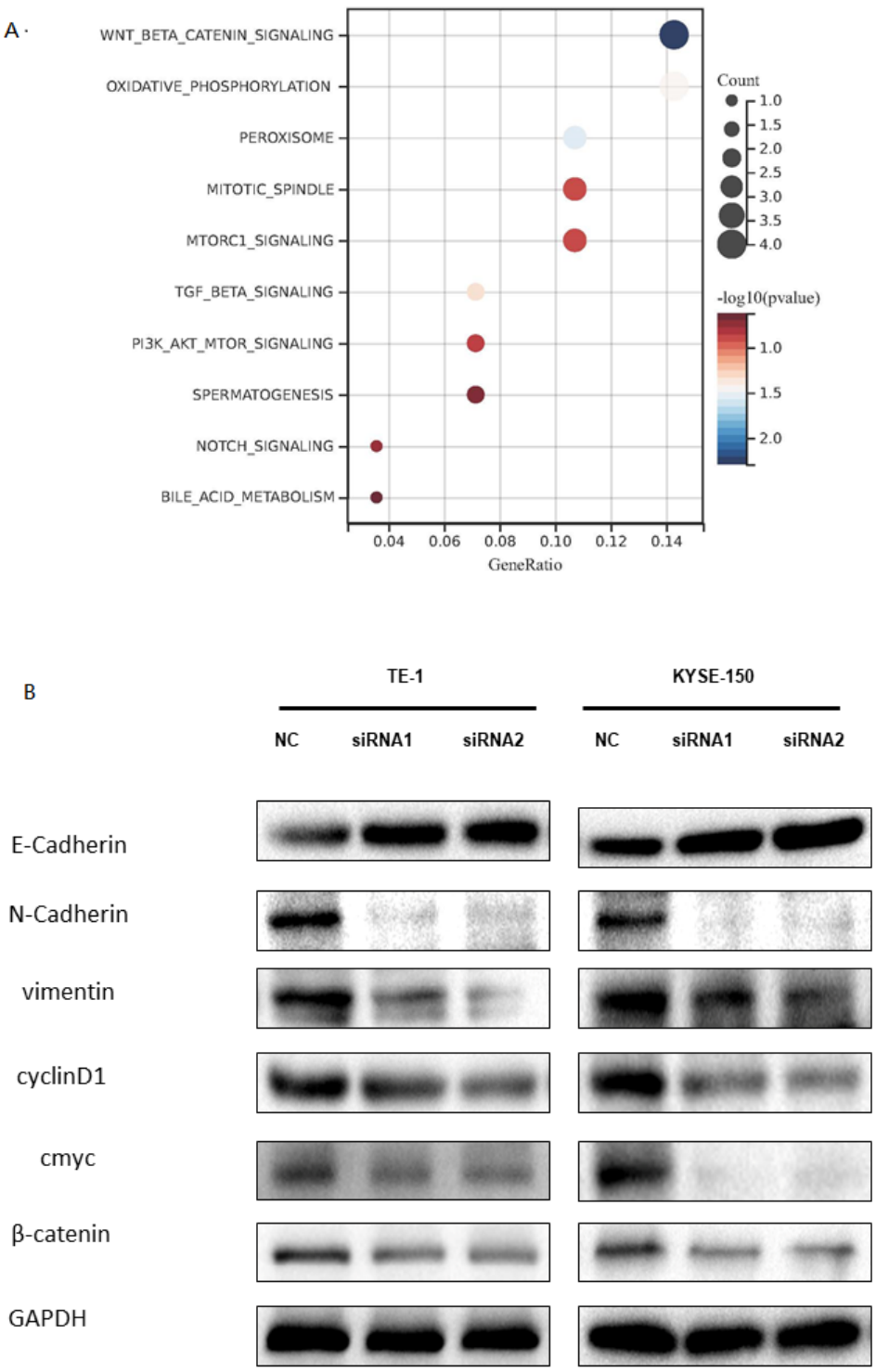

Figure 10

The relationship between ENO1, EMT and Wnt signal pathway. (A)KEGG enrichment analysis; (B) ENO1 promoted EMT of ESCC via the Wnt signal pathway.